IEEE Access
Multidisciplinary | Rapid Review | Open Access Journal

Received July 29, 2020, accepted August 8, 2020, date of publication August 25, 2020, date of current version September 9, 2020.

Digital Object Identifier 10.1109/ACCESS.2020.3019395

Design and Implementation of Time-Domain Interference Cancellation Receiver for LTE-U Systems

TIEN-YU WANG[1,2] **AND TZI-DAR CHIUEH**[1,3]**, (Fellow, IEEE)**
[1]Graduate Institute of Electronics Engineering, National Taiwan University, Taipei 106216, Taiwan
[2]Mediatek Inc., Hsinchu 300096, Taiwan
[3]Department of Electrical Engineering, National Taiwan University, Taipei 106216, Taiwan

Corresponding author: Tzi-Dar Chiueh (chiueh@ntu.edu.tw)

This work was supported in part by the Ministry of Science and Technology, Taiwan, under MOST-104-2221-E-002-075-MY2.

ABSTRACT Mobile devices nowadays have penetrated our daily life and they play a big role in our social, professional, and recreational activities. In order to satisfy the booming demands for mobile communications from their customers, the telecommunication service providers work very hard to secure more spectrum and construct more base-stations. As such, they have looked into unlicensed spectrum for possible deployment of their mobile services. Toward this end, this paper presents a time-domain interference cancellation (TDIC) receiver technique that can enhance the efficiency of mobile communication networks coexisting with Wi-Fi traffic in the unlicensed bands. Moreover, transmitter power control and novel channel estimation are proposed to optimize the overall throughput of the fourth-generation mobile communication networks operating in the unlicensed bands (LTE-U). We further show by simulation and by over-the-air (OTA) real-time demonstration that the proposed solution indeed can achieve reliable reception of LTE-U signals under Wi-Fi interferences with different power levels.

INDEX TERMS Heterogeneous network coexistence, interference cancellation, LTE-U, unlicensed spectrum.

I. INTRODUCTION

According to the statistics from International Telecommunication Union (ITU), on the average up to 103.5 mobile phones are owned by 100 persons by the end of 2017, implying a growing trend of multiple phones by one individual. As wireless technology advances, mobile audio and video streaming services are required to provide better user experience and higher quality. In addition, online media streaming services, such as YouTube, Netflix, etc. are gaining popularity. All the above lead to the explosive growth in wireless data traffic that we have witnessed in the past few years.

Even though the 5G spectrum has been licensed in many countries and 5G mobile services are being launched recently, long term evolution (LTE) is still the most popular cellular communication standard. As such, expanding the spectrum used by LTE mobile communication seems to be a viable solution to tackle the spectrum crowding issue. Many research teams have been working on how to expand the spectrum usage of the LTE services, such as leveraging resources in the unlicensed band [1]–[6]. Among these works, the LTE-unlicensed (LTE-U) and the Licensed Assisted Access (LAA) techniques are currently the most studied approaches and they are also being upgraded to the 5G new radio (NR) standard. The LTE-U scheme adopted the carrier-sensing adaptive transmission (CSAT), while the LAA scheme adopted the listen-before-talk (LBT) technique.

To deploy the LTE traffic in the unlicensed bands, spectrum sharing of the LTE signals with the most popular Wi-Fi signals in the unlicensed bands is inevitable. However, such a task is quite challenging as the LTE signals and their reception are designed for operation in licensed spectrum, where very little unmanaged interference is expected. Consequently, there is no mechanism for collision management in the current LTE standard. Wi-Fi, on the other hand, operates in the unlicensed spectrum that can be accessed by many other wireless devices, so its standard stipulates the Carrier Sense Multiple Access with Collision Avoidance (CSMA/CA) mechanism to manage possible collisions. The main concept of CSMA/CA is to detect channel clearance before the transmitter tries to send data. If the channel is clear, the intended transmission will be permitted; otherwise,

The associate editor coordinating the review of this manuscript and approving it for publication was Zeeshan Kaleem.

the transmission will be postponed until later. If the LTE and the Wi-Fi networks share the same frequency bands without any consideration for collision management from the LTE network, the performance of the Wi-Fi network will be degraded severely [7]. This is because during carrier sensing, the Wi-Fi transmitters almost always find the channel in use by LTE signals. Even if by chance some Wi-Fi transmitter finds the right to use the channel, transmission of Wi-Fi packets can be interrupted by intermittent LTE signals, leading to considerable performance degradation in both networks.

Previously, the concept of *blank subframe* (BS) that blanks out specific LTE subframes was proposed in [8]. This technique allows LTE and Wi-Fi to coexist by exploiting different blank subframe patterns with a certain duty cycle. An LTE frame (10ms long) is composed of ten subframes (1ms each). The blank subframe method will blank out several subframes in one frame, making the channel clear for Wi-Fi transmission in those intervals. Even though this method mitigates the issue of LTE transmitter seizing the channel 100% of the time, the issues of the ratio of blank subframes and the blanking patterns still remain. In [9], [10], the LTE signal duty cycle is adjusted according to the detected interference level and the channel status. However, it is possible that a Wi-Fi packet will transmit beyond the end of the last blank subframes and collide with the following non-blank LTE subframes. In this case, both LTE and Wi-Fi transmission efficiency will deteriorate.

The LBT concept that detects the channel usage before transmitting data was studied in [11]–[14]. This scheme can be further categorized into with or without the *random back-off* mechanism. Specifically, the study in [11] proposed two approaches. In the frame-based equipment (FBE), the channel will be checked during fixed duration of clear channel access (CCA) to decide whether the LTE transmitter should transmit after the end of CCA check. The second approach is load-based equipment (LBE), which is not fixed in time but demand-driven. If the channel is decided to be in the idle state from the CCA check, the LBE can transmit data immediately. Otherwise, an Extended CCA (ECCA) with random back-off is performed, where the channel is observed for the duration of a random integer multiplied by the CCA check time. In [12], an efficient framework for fair coexistence between LTE and Wi-Fi systems was proposed. In that framework, each network has multiple priority classes and both networks can optimize the throughput and latency. Another work proposed to apply modified transmit opportunity (TXOP) in the Wi-Fi system to accommodate coexistence with the LTE network [14]. In this scheme, Wi-Fi devices sense the LTE signal as interference and compute the signal to interference and noise ratio (SINR) to set proper operation mode, modulation order, and code rate. In [15], a temporal coexistence approach was proposed, where it utilizes the point coordination function (PCF) mechanism and the contention free period (CFP) in the Wi-Fi system. All the aforementioned solutions are based on the concept of collision avoidance in the time domain, which will certainly degrade the throughput performance of both the LTE and Wi-Fi systems. This is because, given the non-deterministic nature of the Wi-Fi traffic, it is next to impossible to achieve perfect multiplexing of the two types of traffic without any collision.

Aside from coexistence of LTE and Wi-Fi in the time domain, some researches focused on the frequency-domain coexistence techniques [16], [17]. The author of [16] proposed the low amplitude stream injection (LASI) technique, which injects low amplitude signals to the Wi-Fi sub-carriers to separate the LTE and Wi-Fi signals on the shared spectrum when certain part of their frequency bands overlapped. However, the proportion of the collision between the LTE and Wi-Fi signals is not fixed, which means that LASI has to adjust the collision ratio, and therefore the MAC layer of the Wi-Fi devices. Besides, in the case when the power levels of LTE and Wi-Fi signals are similar, locating the timing of Wi-Fi packets using their preamble signals will be problematic for LASI. The approach proposed in [17] can estimate the channel of LTE or Wi-Fi without clean reference signals, allowing both systems to transmit data at the same location on the same spectrum simultaneously. Nonetheless, the original collision avoidance mechanism in Wi-Fi has to be modified since collision is always allowed in this scheme.

The proposed TDIC technique can effectively handle the collision between LTE-U and Wi-Fi signals, and a TDIC-based LTE physical (PHY) layer receiver mainly consists of three stages: Wi-Fi demodulation, Wi-Fi waveform reconstruction and removal, and LTE demodulation. In the Wi-Fi demodulation stage, the LTE subframe signal power is set relatively lower than that of the colliding Wi-Fi packets, so that the Wi-Fi demodulation works properly. The time-domain Wi-Fi waveform, the interfering component of the received signal at the LTE-U receiver is reconstructed based on the demodulated packets and the estimated Wi-Fi TX to LTE-U RX channel response. Then the LTE-U TDIC-based receiver removes the Wi-Fi component from the received signal and performs the final LTE demodulation. The innovation and contributions of this paper are summarized as follows:

- Propose a receiver with an interference cancellation technique that allows LTE-U and Wi-Fi to collide in the time domain without modifying the original Wi-Fi specification;
- Further improve the effectiveness of TDIC by adopting LTE-U blank subframes and power control; and
- Demonstrate the performance of the TDIC technique by conducting OTA measurements of software-defined radio (SDR) implementation of the LTE-U TDIC-based PHY receiver.

The rest of the paper is organized as follows. Section II introduces the system model used in the unlicensed band LTE-Wi-Fi coexistence scenario. In Section III, the proposed TDIC-based PHY techniques and related design are described. Section IV then shows the simulation results of the TDIC-based PHY receiver performance under different indoor channel scenarios. Section V then presents the OTA

experimental results of the proposed receiver. Several discussions are given in Section VI, and finally Section VII concludes this paper.

II. SYSTEM MODEL

In order to study the issue of coexistence between the LTE and Wi-Fi signals in the unlicensed bands, we consider a scenario where both systems are operating simultaneously. Figure 1 depicts one of the possible scenarios that both an LTE-U base-station (BS) transmitter and another Wi-Fi transmitter are transmitting in the same unlicensed band. The receiver of an LTE-U user equipment (UE) will receive the signals from both sources, which are given by

$$y(t) = h(t) * x(t) + g(t) * z(t) + n(t), \tag{1}$$

where $*$ is the convolution operation; $x(t)$ and $z(t)$ are the LTE transmission signal and the Wi-Fi transmission signal, respectively; $h(t)$ and $g(t)$ are the time-domain channel responses from the LTE transmitter and the Wi-Fi transmitter to the receiver, respectively; and $n(t)$ is all-white Gaussian channel noise.

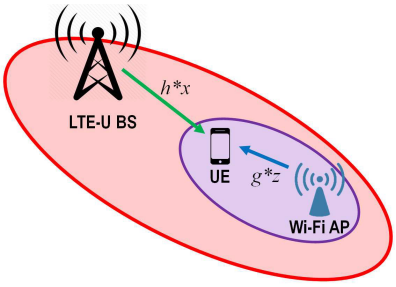

FIGURE 1. A scenario of coexisting LTE and Wi-Fi networks in unlicensed bands.

Note that the LTE signal is an orthogonal frequency division multiplexing (OFDM) signal with a subcarrier spacing of 15KHz, while the Wi-Fi signal is also an OFDM signal yet using a subcarrier spacing of 312.5KHz. Since the subcarrier spacings in these two signals are incompatible, we thus have to model these two signals in the time domain rather than in the frequency domain, as most OFDM systems do.

III. PROPOSED LTE-U TDIC-BASED RECEIVER WITH TRANSMISSION POWER CONTROL

A. POWER CONTROL

Power control is a mature technology that has been used extensively in interference-limited mobile communication networks, such as the 3G CDMA standards. Interference cancellation techniques are also abundant in wireless receiver studies. In this paper, we propose to combine these two techniques with the blank subframe scheme to construct an effective solution to LTE and Wi-Fi coexistence in unlicensed spectrum. For effective interference cancellation, power control must make sure that the interference signal can be detected correctly and then cancelled. Otherwise, with incorrect interference detection, the cancellation step will just inject a more severe error to the receiver processing, making the performance even worse than the case without interference cancellation. To ensure high enough success probabilities of Wi-Fi packet detection and demodulation, we propose to fix the Wi-Fi transmission power and adjust the LTE transmission power so that at the receiving end the power of the Wi-Fi packets and that of the LTE subframes are set to some proper ratio. Define the interference-to-signal ratio (ISR) as

$$\mathrm{ISR(dB)} = 10\log_{10}\frac{P_{\text{Wi-Fi}}}{P_{\text{LTE}}}, \tag{2}$$

where we deem the Wi-Fi signal as the interference and the LTE signal as the intended signal in the LTE-U TDIC-based receiver.

To achieve a high enough successful Wi-Fi packet detection rate, or conversely low enough Wi-Fi packet error rate, we want to maintain a high enough signal to interference and noise ratio (SINR) for the Wi-Fi demodulator. This can be accomplished by making the above ISR higher than, say 9dB. In this case, the Wi-Fi packet demodulation is relatively easy, while the colliding LTE subframes will be overwhelmed by the stronger Wi-Fi signal. However, the LTE-U receiver, with the help of TDIC, can still successfully detect the LTE signal after cancelling the Wi-Fi interference.

B. WI-FI DEMODULATION

Figure 2 depicts the flow chart of the Wi-Fi demodulation used in the proposed receiver. To begin with, the coarse symbol boundary detection (CSBD) and fine symbol boundary detection (FSBD) are carried out by exploiting the repeating property of Wi-Fi packet legacy short training filed (L-STF). With the detection of L-STF, the demodulator can detect the Wi-Fi packet header and locate the starting position of the incoming Wi-Fi packet. With L-STF, which is made up of 10 repeated segments, the demodulator can also estimate the carrier frequency offset (CFO) between the Wi-Fi transmitter and the Wi-Fi demodulator. Another processing step in the demodulator is to compensate the CFO in the time domain by a numerically-controlled oscillator (NCO).

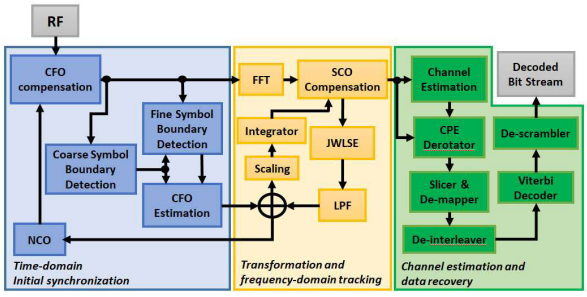

FIGURE 2. Wi-Fi demodulation flow chart.

After the OFDM symbol boundaries are detected, we transform the received time-domain signal into the frequency-domain signal by fast Fourier transform (FFT). Then the channel response from the Wi-Fi transmitter can be estimated using the legacy long-training field (L-LTF) in the packet header. In addition, residual CFO and sampling

clock offset (SCO) can both be estimated based on the received frequency-domain L-LTF signal and the pilot subcarrier signals in the following information-carrying OFDM symbols. Finally, the transmitted information bitstream can be recovered from the equalized frequency-domain signal by the slicer, demapper, de-interleaver, Viterbi error-correcting code decoder, and de-scrambler. For further details of Wi-Fi demodulation, the readers are referred to [18].

In the intended coexistence scenario, the Wi-Fi demodulator needs to deal with LTE signal contamination. As a result, several Wi-Fi demodulation steps have to be modified. The following will describe those blocks that require modification.

1) COARSE SYMBOL BOUNDARY DETECTION

Traditional coarse symbol boundary detection is achieved by detecting the L-STF, also known as short preamble, that comprises 10 repeated segments, each 3.2 μs long. When the Wi-Fi demodulator operates at 20MHz sampling rate, one L-STF segment consists of 16 samples. To detect the 16-sample periodicity, traditional Wi-Fi demodulator computes normalized 16-sample delay correlation and searches for periodic peaks. In the case of LTE-U coexistence, the proposed Wi-Fi demodulator enhances the detection performance by considering both the 16-point delay correlation and the 32-point delay correlation. Fig. 3 depicts the three correlation windows used: two 16-point windows and one 32-point window. Moreover, the estimated DC offset is removed before calculating the delay correlation to suppress false alarms. The computed metrics are listed in (3), (4), (5)

$$c_n = \sum_{k=0}^{l-1} w_{n+k} w^*_{n+k+l} + \sum_{k=0}^{l-1} w_{n+k+l} w^*_{n+k+2l} + \sum_{k=0}^{2l-1} w_{n+k} w^*_{n+k+2l} \tag{3}$$

$$p_n = \sum_{k=0}^{2l-1} \|w_{n+k}\|^2 + \sum_{k=0}^{2l-1} \|w_{n+k+l}\|^2 + \sum_{k=0}^{4l-1} \|w_{n+k}\|^2 \tag{4}$$

$$m_n = \frac{4|c_n|^2}{|p_n|^2}, \tag{5}$$

where l is set to 16; $w_n = y_n - \mu_y$ and μ_y is the average of the corresponding 32-sample window of the received signal y_n, and m_n is the normalized 16-point plus 32-point delay correlation output.

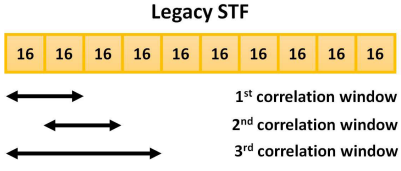

FIGURE 3. Three correlation windows used in the proposed robust Wi-Fi coarse symbol boundary detection.

2) CFO ESTIMATION

Owing to the modification in the CSBD, the estimation of CFO requires some modification as well. Considering only the impact from CFO on the received signal, we can the estimate the fractional CFO as

$$\epsilon = \sum_{k=1}^{15} \frac{\angle c_{b-17-k}}{16 \cdot 2\pi}, \tag{6}$$

where b is the index that indicates the position where the normalized 16-point plus 32-point delay correlation output drops below a predefined threshold after reaching a plateau, which represents the end of L-STF, and $|\angle c_{b-17-k}| < 2\pi$.

C. WI-FI WAVEFORM RECONSTRUCTION AND CANCELLATION

With the information bitstream successfully decoded from a Wi-Fi packet, we then need to reconstruct the Wi-Fi component in the received time-domain signal in order to cancel the Wi-Fi interference. To this end, we start with the transmitted time-domain baseband waveform of the Wi-Fi packet, generated by a baseband Wi-Fi modulator. Then, pass the baseband waveform through a software model that emulates the effects of the RF circuits of the transmitter and the receiver, plus the channel between the transmitting and receiving antennas. These effects will be described in the following.

1) POWER AMPLIFIER NON-LINEARITY

In the OTA experiments, non-ideal effects such as power amplifier non-linearity at the transmitter should be taken into consideration. Specifically, almost all RF power amplifiers have the gain compression effect, which makes the signals of different magnitudes be amplified differently [19]. Therefore, we have to take this effect into consideration when reconstructing the waveform for cancellation. Basically, there are two kinds of non-linear PA effects: the AM/AM effect and the AM/PM effect. These are the effects that change the baseband signal magnitude and phase, respectively. In this work, we only considered the AM/AM effect since it has more significant impact on correctly cancelling the Wi-Fi interference. The formula for the AM/AM effect is given by

$$A(r) = \frac{v_a r}{\left[1 + (v_a r / A_0)^{2p}\right]^{1/2p}} \tag{7}$$

where r is the input magnitude; v_a is the small-signal gain; A_0 and p are parameters for the PA. In our OTA implementation, we determined the optimal parameter settings according to the measurement results to further enhance the effectiveness of the Wi-Fi interference cancellation.

2) CHANNEL ESTIMATION WHEN WI-FI OVERLAPS LTE-U

Since we adopted the blank subframe technique, several subframes are muted in each LTE frame, and the Wi-Fi transmitters can operate during these blank intervals. Unfortunately, the tail part of a Wi-Fi packet may still collide with the non-blank LTE subframes. We call the Wi-Fi packets

completely within a blank subframe interval *clean* packets, and call those that have a portion of the packets colliding with LTE signal *contaminated* packets. For clean packets, it is relatively easy to implement channel estimation and signal demodulation. On the other hand, contaminated packets may have difficulty in achieving channel estimation if its L-LTF is fully or partially contaminated. To help deal with this situation, we resorted to the fact that temporally nearby packets are likely transmitted by the same device. As such, we assumed that consecutive packets experience similar channel, and used the estimated channel responses of the nearest clean packet for the contaminated packet. However, straightforward application of the above idea led to poor estimation performance.

In Figure 4, we plot the phases of the channel frequency responses (CFR) of the L-LTF parts of six consecutive measured packets in an over-the-air experiment. Phase responses 1, 2, and 3 belong to three clean Wi-Fi packets, while 4, 5, and 6 are associated with Wi-Fi packets colliding with LTE subframes. We noticed that the CFR phase differences between adjacent clean packets are proportional to the subcarrier indices, implying even temporally nearby clean packets do not have similar CFR phase responses. Referring to [19], we postulated that this phenomenon is due to possible symbol timing offset leading to FFT windows in different packets covering cyclic shifted version of the L-LTF. The linear phase shift of the CFR is clear from the following CFR estimation formula

$$Y_l[k] = \frac{1}{N}\sum_{n=0}^{N-1} x_l[n+\delta]e^{-j2\pi nk/N} = X_l[k]e^{j2\pi k\delta/N}, \quad (8)$$

where Y_l and X_l are the estimated and true CFRs, and δ is the timing offset. In light of the above analysis, even the adjacent clean packets do not have identical CFRs, but rather their CFRs differ slightly due to linear phase shift caused by symbol timing offset. Consequently, replacing the CFR of a contaminated packet by that of a temporally nearby clean packet is not applicable unless the timing offset effect is properly dealt with.

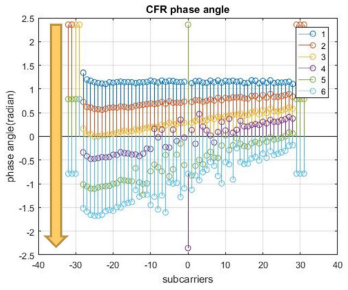

FIGURE 4. Phases of estimated channel frequency responses of six consecutive measured Wi-Fi packets.

For packets 4, 5, and 6, collision with the LTE signal makes CFR phases relatively noisy, leading to poor demodulation outcomes in these packets. To obtain proper CFR for a contaminated packet, we proposed to begin with the CFR of an adjacent clean packet; determine the optimal phase shift slope and then derive the CFR of the contaminated packet accordingly. Take packet 4 as an example, we computed the phase difference between CFRs of packets 3 and 4; then found a noise-free regression line, as shown in Figure 5(a). Finally, we combined the CFR of packet 3 and the regressed phase difference line (due to timing offset between two packets) to obtain the estimated CFR of packet 4, as shown in Figure 5(b). Figure 6 shows the real part of the estimated channel impulse response (CIR) of packet 4. It is clear that after removing the effects from interference and timing offset, the CIR of packet 4 looks just like a single-tap channel for indoor environments.

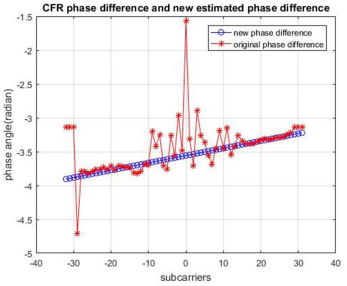

(a)

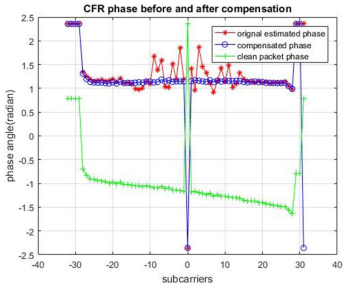

(b)

FIGURE 5. (a) CFR phase difference before and after linear regression, and (b) CFR phase before and after timing offset compensation.

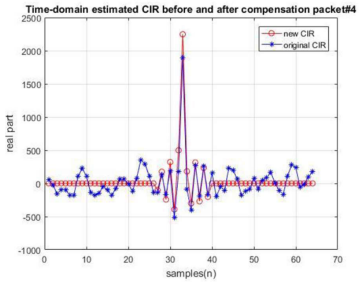

FIGURE 6. Estimated channel impulse response (CIR) of the contaminated packet before and after timing offset compensation.

For clarity, we list the pseudo-code for Wi-Fi channel estimation (specifically for Wi-Fi packets that overlap with LTE subframes) in Algorithm 1. In addition, the whole TDIC procedure is depicted in Fig. 7, which includes channel frequency response estimation via linear regression, channel impulse response generation, channel effect, PA non-linearity

Algorithm 1: Wi-Fi Waveform Reconstruction

Input: Detected Wi-Fi packet **P**, Channel Frequency Response **H**
Output: Reconstructed Wi-Fi waveform $\widetilde{W}_i$
for $i = 1$ ***to*** n ***packet detected*** **do**
  Demodulate $p_i \in P$ to receive bitstream b_i
  Generate the waveform W_i according to b_i
  if p_i *is contaminated* **then**
    Find the nearest preceding clean packet c_j
    $\Delta H_{i,j} \leftarrow H_{p_i} - H_{c_j}$
    Use linear regression to find a line $\Delta H_{i,j,reg}$ to replace $\Delta H_{i,j}$
    $H_{p_i'} \leftarrow H_{c_j} + \Delta H_{i,j,reg}$
    $h_{p_i'} \leftarrow IFFT(H_{p_i'})$
    $\widetilde{W}_i \leftarrow W_i * h_{p_i'}$
  end
  else
    $h_{p_i} \leftarrow IFFT(H_{p_i})$
    $\widetilde{W}_i \leftarrow W_i * h_{p_i}$
  end
end

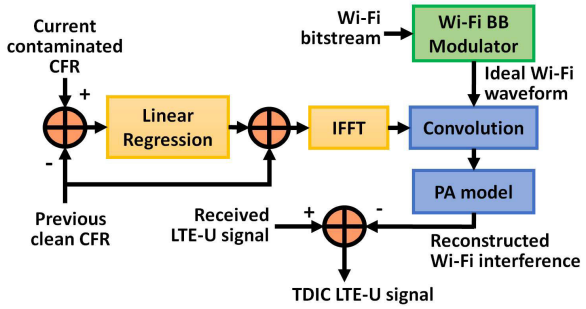

FIGURE 7. Signal flow chart of the proposed time-domain interference cancellation (TDIC) technique.

effect, and finally cancellation of the reconstructed Wi-Fi interference from the received LTE-U signal.

D. LTE DEMODULATION

LTE demodulation basically has three steps just as Wi-Fi demodulation: (1) time-domain initial synchronization (2) transformation and frequency-domain tracking, and (3) channel estimation and data recovery. The main differences between them are: (1) synchronization of the Wi-Fi signal is carried out by exploiting its repeating preamble segments, while for the LTE signal, primary synchronization sequence (PSS) and secondary synchronization sequence (SSS) are used to achieve synchronization and determine the cell ID. (2) For forward-error-correction (FEC) decoding, the convolutional decoder is adopted in the Wi-Fi system, while the turbo decoder is adopted in the LTE system. For details of LTE demodulation, please refer to [20].

IV. SIMULATION RESULTS

In this section, the simulation results of an LTE-U receiver inside a Wi-Fi service region that overlaps an LTE cell (as shown in Figure 1) are presented. Table 1 lists the simulation parameters used. The LTE base-station and the Wi-Fi transmitters both adopt a single antenna to transmit signals, and the modulation for LTE is QPSK while the modulation and coding scheme (MCS) for Wi-Fi is set to 0. The Wi-Fi TGn channel model A is adopted and the simulated SNR for the Wi-Fi signal is 18dB – 25dB with ISR set to 3, 6, 9, 12, and 15dB. We set the Wi-Fi signal to a fixed power level, and adjusted the power levels of the noise and the LTE signal to obtain required Wi-Fi SNR and ISR, respectively. Figure 8 illustrates the simulated block error rate (BLER) versus Wi-Fi SNR of the LTE-U TDIC-based receiver with different ISR levels. When the Wi-Fi SNR is below or equal to 20dB, the minimum LTE BLER is achieved at 6dB ISR. On the other hand, when the Wi-Fi SNR is higher than or equal to 21dB, the minimum BLER is obtained when the ISR is 9dB or 12dB. In all Wi-Fi SNR levels, the TDIC receiver works best when the ISR is within 6-12dB. At ISR level outside this range, LTE-U receiver does not work well.

TABLE 1. LTE-U TDIC-based receiver simulation parameters.

Parameter	*Setting*
LTE modulation	QPSK
LTE bandwidth	10MHz
Wi-Fi MCS	0
Wi-Fi bandwidth	20MHz
Wi-Fi PSDU Length	144bytes
RF frequency	2.5GHz
Sampling rate	20MHz
ISR(dB)	3, 6, 9, 12, 15
SNR(dB)	14 – 25

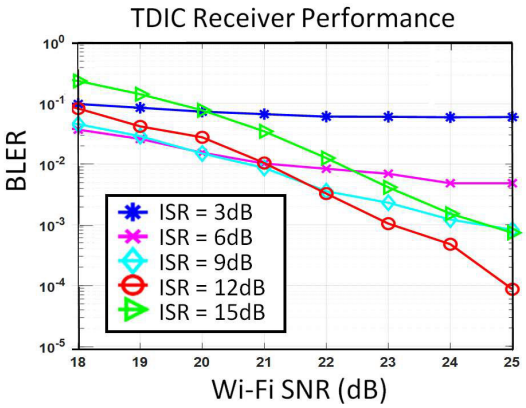

FIGURE 8. LTE-U TDIC-based receiver BLER versus Wi-Fi SNR at different ISR levels.

On the other hand, we can let the horizontal axis be the LTE SNR, namely shifting each curve in Figure 8 according to respective ISR. We then end up with the BLER curves depicted in Figure 9, where the error floor can be observed for low ISR cases. This is because when the LTE SNR increases,

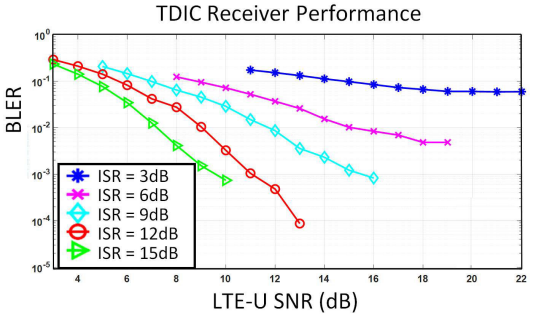

FIGURE 9. LTE-U TDIC-based receiver BLER versus LTE-U SNR at different ISR levels.

the residual Wi-Fi signal that is not cancelled completely will dominate the BLER of the TDIC-based receiver. When the ISR is relatively low, Wi-Fi demodulation often fails and thus interference cancellation does not work, leading to high BLER for LTE signal. On the other extreme, when ISR is high, e.g. 15dB or higher, even with perfect Wi-Fi packet demodulation, small variation in channel and/or small error in channel estimation can lead to considerable residual Wi-Fi signal after interference cancellation and thus an elevated error curve in Figure 8.

To investigate further, we re-plot the LTE-U TDIC-based receiver BLER versus ISR under several Wi-Fi SNR values as shown in Figure 10. It is clear that the performance of LTE-U TDIC-based receiver is highly dependent on proper power control to set the optimal ISR. As mentioned previously, either high or low ISR will degrade the BLER performance of the proposed LTE-U receiver. As the Wi-Fi SNR level changes, the optimal ISR also shifts. However, in all Wi-Fi SNR levels, the BLER curves are convex and bowl-shaped, indicating single optimal ISR. Finally, in the Wi-Fi SNR range of Figure 10, the optimal ISR is within the 7dB – 10dB interval.

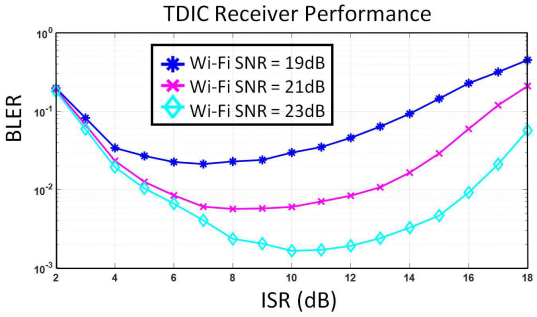

FIGURE 10. LTE-U TDIC-based receiver BLER versus ISR at different Wi-Fi SNR levels.

V. OVER-THE-AIR EXPERIMENTS

A. HARDWARE SETUP

We built an over-the-air demonstration platform to validate the proposed LTE-U and Wi-Fi coexistence solution. In this platform, we adopted the USRP devices from National Instruments as the RF frontend, where the LTE-U and Wi-Fi signals were transmitted by two USRP 2943 respectively. Then both signals were received by the third USRP 2943 working as the RF frontend of the LTE-U receiver. The RF signal carrier frequency is 2.5GHz; the LTE signal bandwidth is 10 MHz; the Wi-Fi signal bandwidth is 20 MHz; and the sampling rate at the baseband receiver is 20 MHz. The rest of the parameter settings are as those in Table 1.

B. EXPERIMENT DESIGN

Figure 11 depicts details about the two transmitters and the LTE-U TDIC-based receiver for the OTA experiment. Due to the different sampling rates of the two baseband signals, the lower-bandwidth LTE baseband signal to be transmitted was up-sampled to 20 MHz before proceeding to power control, where the power levels of the two signals were adjusted to set the required ISR level. The receiver RF frontend down-converted the received RF signal into baseband I/Q signals and fed them to the TDIC-based baseband processing blocks. In the TDIC-based baseband receiver, the Wi-Fi demodulation block first detected the Wi-Fi packet's header, if any, and then performed CFO detection, channel estimation, OFDM demodulation, and FEC decoding. Next, the demodulated Wi-Fi bitstream was passed to the Wi-Fi waveform reconstruction block consisting of a Wi-Fi baseband modulator and channel effect processing emulating the power amplifier nonlinearity and OTA channel effects. The reconstructed Wi-Fi waveform was cancelled from the received waveform and the resulting waveform was down-sampled to the nominal sample rate of the 10-MHz-bandwidth LTE signal for the final demodulation.

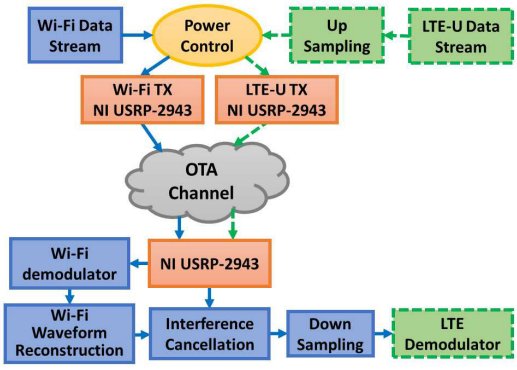

FIGURE 11. Over-the-air (OTA) experiment flow chart.

C. MEASUREMENT RESULTS

Figure 12 illustrates several key results of the proposed TDIC-based receiver when receiving the OTA Wi-Fi and LTE-U signals. Figure 12(a) shows the received waveform before TDIC, where the signal with stronger power is the Wi-Fi signal and the LTE-U signal shows clear blank subframes. It is obvious that with power control setting proper ISR value, the Wi-Fi packets become relatively strong interference, thereby facilitating successful demodulation of the Wi-Fi packets. Next, the demodulated Wi-Fi bitstream is reconstructed into the corresponding time-domain waveform with corresponding RF frontend and channel effects.

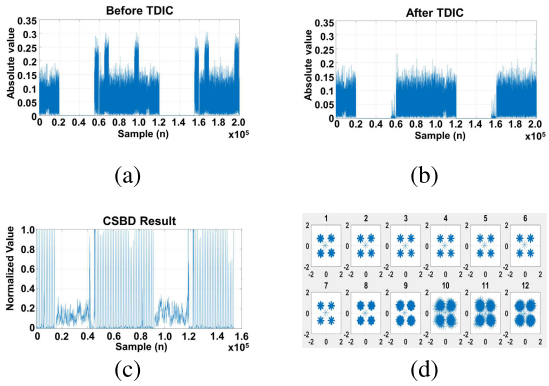

FIGURE 12. Key signal waveforms and reconstructed constellations of the TDIC-based receiver: (a) waveform before applying TDIC, (b) waveform after applying TDIC, (c) LTE CSBD result after applying the TDIC. (d) equalized constellations of the LTE-U signal after TDIC.

The resulting waveform is removed from the received waveform and the interference cancelled signal waveform is shown in Figure 12(b). Note that the TDIC technique cannot completely remove the Wi-Fi component in the received signal, as is clearly seen in the blank subframe intervals where some residual Wi-Fi signals exist. The effect of the residual Wi-Fi signal on the LTE demodulation is then evaluated by plotting the LTE coarse symbol boundary detection (CSBD) outcome in Figure 12(c). Note that Figures 12(a)(b) both depict a 10ms interval and each has 200,000 samples with 20MHz sample rate, while Figure 12(c) has only 153,600 samples as the interference cancelled waveform has been down-sampled to 15.36MHz. The normalized delayed correlation values of the LTE-U signal contaminated by Wi-Fi packets are relatively lower due to incomplete Wi-Fi interference cancellation. However, the decrease in CSBD peaks is still within the receiver detection margin and all LTE-U symbols are detected.

To illustrate the degree of adverse effect brought about by the Wi-Fi residual signal, we plot the equalized OFDM signals of 12 LTE-U symbols with extended cyclic prefix in Figure 12(d). Apparently, despite coexisting with Wi-Fi packets, the LTE-U signal can be effectively detected by the proposed LTE-U TDIC-based receiver and in all symbols the equalized constellations are quite distinct, implying good bit error rate outcome. Symbols 10 – 12 correspond to the interval that overlaps a Wi-Fi packet, and the SNR of their equalized signals thus becomes poorer due to the residual Wi-Fi signal.

D. POWER CONTROL EFFECT

To further validate the previous simulation results about the power control effect, we conducted the OTA experiments for different ISR values. Figure 13 depicts the OTA reception BLER results of the proposed LTE-U TDIC-based receiver for different ISR values. All three curves corresponding to different Wi-Fi SNR values show a concave trend similar to the simulation results in Figure 10. Increasing ISR from 2dB allows Wi-Fi packets to be removed more completely, giving

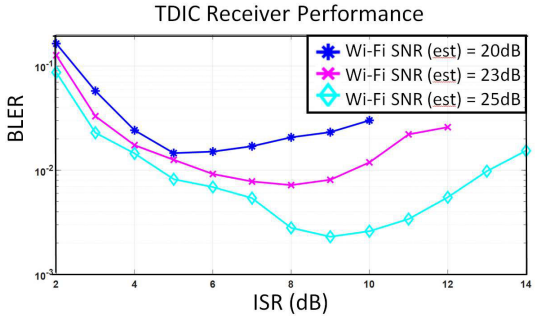

FIGURE 13. LTE-U BLER performance with different ISR by the proposed TDIC-based receiver in the OTA experiment.

better LTE BLER. As ISR keeps increasing, the impact of the Wi-Fi residue becomes relatively stronger than the weaker and weaker LTE-U signal, and at some point the LTE BLER stops decreasing and starts to increase. Moreover, similar to the simulated results in Figure 10, the BLER improves as the Wi-Fi SNR gets better and the optimal ISR also increases because weaker LTE-U signal can still be detected as the noise gets smaller.

E. GPU-ACCELERATED REAL-TIME RECEIVER

To demonstrate real-time reception, the proposed LTE-U TDIC-based receiver was ported a GPU card (NVIDIA GTX1080Ti) mounted on a host computer. In this real-time SDR solution, in order to be able to perform real-time demodulation, previous baseband receiver was converted to OpenCL, a programming language for heterogeneous computing environment consisting of, e.g., CPU and GPU. Many of the signal processing blocks in the proposed baseband receiver are inherent parallel and can leverage the excellent parallel processing capabilities of the adopted GPU. Therefore, the execution time for the LTE-U TDIC-based receiver was greatly reduced, by more than an order of magnitude.

The received and down-converted baseband in-phase and quadrature-phase (I/Q) signals were partitioned into 40ms segments (four LTE frames). Each segment was processed by the CPU and GPU for Wi-Fi packet detection, Wi-Fi demodulation, Wi-Fi waveform reconstruction, time-domain interference cancellation, and finally LTE OFDM demodulation. On average, the total execution time was about 16.4ms, which is more than fast enough for real-time OTA reception demonstration.

Figure 14 illustrates the effect of LTE-U blank subframe ratio on the reception performance via a graphical user interface (GUI). In this experiment, the ISR was set at about 9dB for optimal power control and thus all Wi-Fi packets were successfully demodulated. In the example of Figure 14(a) with 2 out of 10 subframes being blank, all Wi-Fi packets collided with LTE-U subframes because of low BS ratio. Furthermore, there was no preceding clean Wi-Fi packets, from which the channel information of the interfering transmitter can be reliably estimated. Hence Wi-Fi waveform reconstruction and time-domain interference

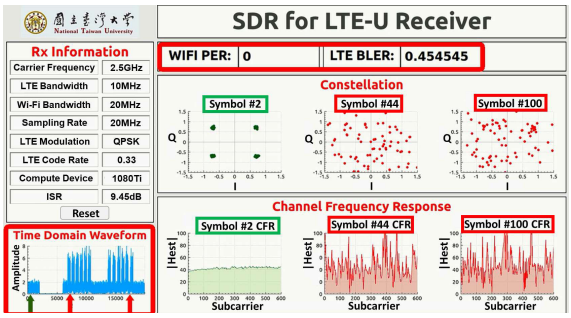

(a)

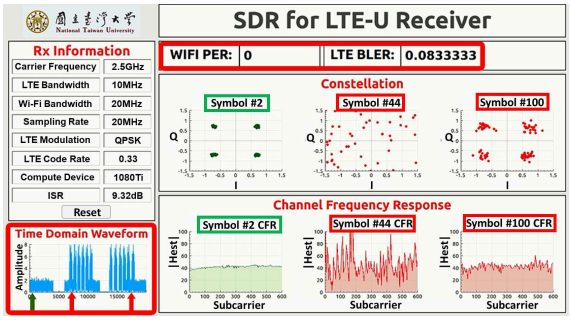

(b)

FIGURE 14. Impact of blank subframe (BS) ratio on LTE-U TDIC-based receiver performance using the GPU-based OTA SDR platform: (a) BS ratio is 2 out of 10 (b) BS ratio is 4 out of 10. Green arrows indicate clean LTE signal regions; red arrows refer to LTE and Wi-Fi collision regions.

cancellation failed, resulting in very poor LTE-U demodulation performance.

With the BS ratio increased to 4 out of 10 subframes being blank, as shown in Figure 14(b), some Wi-Fi packets were free of collision and helped the following contaminated packets in obtaining more accurate channel information. Therefore, the time-domain interference cancellation technique was more effective. However, there were still some contaminated packets with no clean packet for assistance in channel estimation and thus had poor LTE-U demodulation performance, e.g., symbol #44 in Figure 14(b). In contrast, symbol #100, though also interfered by a Wi-Fi packet as symbol #44, enjoyed the help from the preceding clean packet in channel estimation and thus have good estimated CFR (as those in symbol #2). In addition, its equalized constellation and BLER were both much improved than those of symbol #44.

In summary, the effectiveness of the proposed channel estimation, power control, non-linearity compensation, and time-domain interference cancellation techniques has been clearly validated by the real-time OTA experiments. A demonstration video of these OTA experiments is available at https://www.youtube.com/watch?v=3zyNEwB4IPc

VI. DISCUSSIONS

Previous studies on ISM band coexistence are mainly based on the LBT technique or duty cycle management. They are mostly designed with a view to collision avoidance or collision resolution, as shown in Table 2. As far as we know,

TABLE 2. Comparison of LTE-U techniques.

	Work with collision	Medium sensing	Wi-Fi protocol modification
Channel sensing	No	Yes	No
LBT	No	Yes	No
Duty cycle	No	No	No
CSAT	No	Yes	No
LASI [15]	Yes	No	Yes
[16]	Yes	No	Yes
TDIC	Yes	No	No

the proposed TDIC-based solution is the only one that tries to mitigate the impacts of collision by salvaging the LTE-U signal that has been hit by Wi-Fi packets. In addition, the proposed solution does not require modifying the Wi-Fi protocol. With the proposed technique, LTE blank subframe duty cycle can be reduced without degrading LTE demodulation performance, thus improving the overall throughput. In the event that the TDIC-based receiver fails to recover LTE bitstream, the solution then falls back to the blank subframe method, where only clean LTE subframes can be demodulated. Power control is another advantage in the proposed solution. With this technique, the LTE-U base-station transmitter can optimize the TDIC performance by setting the ISR at the LTE-U receiver. As a result, compared to a traditional LTE receiver, the proposed TDIC-based receiver not only has lower BLER, but also achieves higher throughput.

In this work, we considered a scenario with one LTE base-station, one interfering Wi-Fi transmitter, and one LTE-U receiver. Hence the receiver will only receive Wi-Fi packets from one transmitter, which allows channel estimation for contaminated packets to be carried out by exploiting the information from clean packets. However, if the scenario is extended to a case with multiple Wi-Fi transmitters, the first issue that comes to mind is that we do not know if the temporally nearby clean packets come from the same transmitter as the contaminated packet. For the case that the clean packets come from the same source, TDIC-based receivers still work fine. On the other hand, if the clean packets come from different transmitters, the LTE-U receiver cannot apply the aforementioned technique to reliably demodulate the contaminated packets. To this end, the LTE-U receiver can construct a table of estimated channel responses from clean packets transmitted by active Wi-Fi devices and their corresponding IDs. With this information, the receiver can demodulate the contaminated packets with the help of the clean packet ID and the corresponding stored channel information.

According to our monitoring on Wi-Fi traffic served by an access point (AP), Wi-Fi packets from the same Wi-Fi device usually appear in bursts, especially during streaming traffic. This phenomenon is also observed in [21], where the authors analyzed the performance of Wi-Fi data burst transmission. As such, we believe that the proposed TDIC technique is applicable and effective in actual coexistence scenarios, where bursty Wi-Fi traffic abounds.

VII. CONCLUSIONS

In this paper, we proposed a new coexistence receiver technique: time-domain interference cancellation (TDIC), which can effectively improve the overall throughput of heterogeneous networks where two types of traffic coexist. Unlike the approaches that adopted listen before talk or only duty cycle management technique, the proposed TDIC-based receiver demodulates the interfering Wi-Fi signal and cancels the reconstructed time-domain Wi-Fi waveform to achieve reliable LTE-U signal reception. Numerical simulations confirmed that TDIC can apply in different indoor channel scenarios and the transmission performance can be further improved by transmit power control that operates the receiver in the optimal ISR region. Additionally, we have built an over-the-air platform to validate the proposed technique in an actual heterogeneous network environment. Meanwhile, we implemented a real-time LTE-U TDIC-based receiver in a parallel software accelerated by GPU, which convincingly demonstrated the effectiveness of the proposed TDIC solution in successful reception of LTE-U signal under Wi-Fi interference. In conclusion, we believe that the proposed TDIC-based receiver design together with the power control technique constitutes a very effective and efficient solution to LTE-U receivers in coexistence with Wi-Fi traffic.

REFERENCES

[1] X. Wang, S. Mao, and M. X. Gong, "A survey of LTE Wi-Fi coexistence in unlicensed bands," *GetMobile: Mobile Comput. Commun.*, vol. 20, no. 3, pp. 17–23, Jan. 2017.

[2] A. M. Voicu, L. Simić, and M. Petrova, "Survey of spectrum sharing for inter-technology coexistence," 2017, *arXiv:1712.08589*. [Online]. Available: http://arxiv.org/abs/1712.08589

[3] Qualcomm Technologies. *Making the Best Use of Unlicensed Spectrum*. Accessed: Feb. 2015. [Online]. Available: https://www.qualcomm.com/documents/making-best-use-unlicensed-spectrum-presentation/

[4] Global mobile Suppliers Association (GSA). *LTE in Unlicensed and Shared Spectrum: Trials, Deployments and Devices*. Accessed: Jul. 2019. [Online]. Available: https://gsacom.com/paper/unlicensed-shared-spectrum-report-july-2019/

[5] Qualcomm Technologies, Inc., "LTE in unlicensed spectrum: Harmonious coexistence with Wi-Fi," Qualcomm Technol., San Diego, VA, USA, White Paper, Jun. 2014.

[6] *Study on Licensed-Assisted Access to Unlicensed Spectrum (Release 13)*, 3GPP document TR 36.889 V13.0.0, Jun. 2015.

[7] T. Nihtila, V. Tykhomyrov, O. Alanen, M. A. Uusitalo, A. Sorri, M. Moisio, S. Iraji, R. Ratasuk, and N. Mangalvedhe, "System performance of LTE and IEEE 802.11 coexisting on a shared frequency band," in *Proc. IEEE Wireless Commun. Netw. Conf. (WCNC)*, Shanghai, China, Apr. 2013, pp. 1038–1043.

[8] E. Almeida, A. M. Cavalcante, R. C. D. Paiva, F. S. Chaves, F. M. Abinader, R. D. Vieira, S. Choudhury, E. Tuomaala, and K. Doppler, "Enabling LTE/WiFi coexistence by LTE blank subframe allocation," in *Proc. IEEE Int. Conf. Commun. (ICC)*, Jun. 2013, pp. 5083–5088.

[9] A. K. Sadek, T. Kadous, K. Tang, H. Lee, and M. Fan, "Extending LTE to unlicensed band-Merit and coexistence," in *Proc. IEEE Int. Conf. Commun. Workshop (ICCW)*, London, U.K., Jun. 2015, pp. 2344–2349.

[10] Y. Jian, U. P. Moravapalle, C.-F. Shih, and R. Sivakumar, "Duet: An adaptive algorithm for the coexistence of LTE-U and WiFi in unlicensed spectrum," in *Proc. Int. Conf. Comput., Netw. Commun. (ICNC)*, Santa Clara, CA, USA, Jan. 2017, pp. 19–25.

[11] ETSI, *5 GHz RLAN; Harmonised Standard Covering the Essential Requirements of Article 3.2 of Directive 2014/53/EU*, Harmonized European Standard ETSI EN 301 893 V2.1.1, May 2017.

[12] M. Hirzallah, M. Krunz, and Y. Xiao, "Harmonious cross-technology coexistence with heterogeneous traffic in unlicensed bands: Analysis and approximations," *IEEE Trans. Cognit. Commun. Netw.*, vol. 5, no. 3, pp. 690–701, Sep. 2019.

[13] K. Yoon, T. Park, J. Kim, W. Sun, S. Hwang, I. Kang, and S. Choi, "COTA: Channel occupancy time adaptation for LTE in unlicensed spectrum," in *Proc. IEEE Int. Symp. Dyn. Spectr. Access Netw. (DySPAN)*, Mar. 2017, pp. 1–10.

[14] M. Hirzallah, W. Afifi, and M. Krunz, "Full-Duplex-Based Rate/Mode adaptation strategies for Wi-Fi/LTE-U coexistence: A POMDP approach," *IEEE J. Sel. Areas Commun.*, vol. 35, no. 1, pp. 20–29, Jan. 2017.

[15] Q. Chen, G. Yu, H. M. Elmaghraby, J. Hamalainen, and Z. Ding, "Embedding LTE-U within Wi-Fi bands for spectrum efficiency improvement," *IEEE Netw.*, vol. 31, no. 2, pp. 72–79, Mar./Apr. 2017.

[16] H. Sun, Z. Fang, Q. Liu, Z. Lu, and T. Zhu, "Enabling LTE and WiFi coexisting in 5 GHz for efficient spectrum utilization," *J. Comput. Netw. Commun.*, vol. 2017, Feb. 2017, Art. no. 5156164.

[17] S. Yun and L. Qiu, "Supporting WiFi and LTE co-existence," in *Proc. IEEE Conf. Comput. Commun. (INFOCOM)*, Hong Kong, Apr. 2015, pp. 810–818.

[18] Z.-Y. Ding, C.-Y. Chen, and T.-D. Chiueh, "Design of a MIMO-OFDM baseband receiver for next-generation wireless LAN," in *Proc. IEEE Int. Symp. Circuits Syst.*, May 2006, p. 4.

[19] T. D. Chiueh, P. Y. Tsai, and I. W. Lai, *Baseband Receiver Design for Wireless MIMO-OFDM Communications*, 2nd ed. Hoboken, NJ, USA: Wiley, Apr. 2012.

[20] J. Demel, S. Koslowski, and F. K. Jondral, "A LTE receiver framework using GNU radio," *J. Signal Process. Syst.*, vol. 78, no. 3, pp. 313–320, Mar. 2015.

[21] I. Tinnirello and S. Choi, "Efficiency analysis of burst transmissions with block ACK in contention-based 802.11e WLANs," in *Proc. IEEE Int. Conf. Commun. (ICC)*, vol. 5, May 2005, pp. 3455–3460.

TIEN-YU WANG was born in Pingtung, Taiwan, in 1994. He received the B.S. degree in electrical engineering from National Cheng-Kung University, in 2016, and the M.S. degree in electronics engineering from National Taiwan University, in 2018.

He is currently with Mediatek, Inc. His research includes LTE-U system design and baseband receiver design.

TZI-DAR CHIUEH (Fellow, IEEE) was born in Taipei, Taiwan, in 1960. He received the B.S.E.E. degree from the National Taiwan University, Taipei, in 1983, and the M.S. and Ph.D. degrees in electrical engineering from the California Institute of Technology, Pasadena, CA, USA, in 1986 and 1989, respectively.

Since 1989, he has been with the Department of Electrical Engineering, National Taiwan University, where he is currently a Distinguished Professor. From 2004 to 2007, he was the Director of the Graduate Institute of Electronics Engineering, National Taiwan University. He has held visiting positions at ETH Zurich Switzerland, from 2000 to 2001, and the State University of New York at Stony Brook, from 2003 to 2004. From November 2010 to January 2014, he served as the Director General of the National Chip Implementation Center, Hsinchu, Taiwan. He also served as the Vice President of National Applied Research Laboratories, from 2015 to 2017. His research interests include IC design for digital communication systems, neural networks, and signal processing for bio-medical systems.

Prof. Chiueh was a recipient of the Outstanding Research Award from National Science Council, Taiwan, from 2004 to 2007. He received the Outstanding Electrical Engineering Professor from the Chinese Institute of Electrical Engineers, Taiwan, in 2005, the Himax Chair Professorship at NTU, in 2006, the Outstanding Industry Contribution Award from the Ministry of Economic Affairs, Taiwan, in 2009, and the Outstanding Technology Transfer Contribution Award from Ministry of Science and Technology, Taiwan, in 2016. His teaching efforts were recognized eleven times by the Teaching Excellence Award from NTU.